Journal of Applied Polymer Science

Graft copolymerization of acrylic acid on to styrene butadiene rubber (SBR) to improve morphology and mechanical properties of SBR/polyurethane blend

Shahed Taheri,[1] Yones Hassani,[2] Gity Mir Mohamad Sadeghi,[3] Fathollah Moztarzadeh,[4] Mei-Chun Li[5]

[1]Department of Biomedical Engineering, Amirkabir University of Technology, Tehran, Iran
[2]Mahshahr Capmus, Amirkabir University of Technology, Mahshahr, Iran
[3]Department of Polymer Engineering & Color Technology, Amirkabir University of Technology, P.O. Box 15875/4413, Tehran, Iran
[4]Biomaterials Group, Department of Biomedical Engineering (Center of Excellence), Amirkabir University of Technology, P.O. Box 15875/4413, Tehran, Iran
[5]School of Renewable Natural Resources, Louisiana State University Ag Center, Baton Rouge Louisiana, 70803
Correspondence to: G. M. M. Sadeghi (E-mail: gsadeghi@aut.ac.ir)

ABSTRACT: Graft copolymerization of acrylic acid (AA) on to styrene butadiene rubber (SBR) is carried out via free radical polymerization using benzoyl peroxide (BPO) as initiator. Graft yield (*GY*) and graft efficiency (*GE*) measurements reveal that the optimum grafting is achieved when 100 wt % of AA and 3 wt % of BPO are used for a reaction time of 6 h at 60 °C. The execution of the grafting process is confirmed through ATR-IR spectroscopy and DMTA analysis. Tan δ thermograms indicate that the graft copolymerization occurs in the styrene segments of the SBR backbone. An *in situ* polymerized, semicrystalline polyurethane (PU) is then used to prepare a series of SBR-g-PAA/PU blends. It is found that the SBR-g-PAA with the highest GY exhibits the best compatibility with PU matrix. One-phase morphology (SEM), as well as the appearance of only one glass transition (DMTA) verify the homogeneous miscibility of the modified blend compositions. Moreover, the integration of PUs crystalline structure into blends gives rise to elongation-induced crystallinity as the prominent phenomenon in tensile testing, which proves to synchronously enhance tensile strength, modulus, elongation at break, and toughness. © 2016 Wiley Periodicals, Inc. J. Appl. Polym. Sci. **2016**, *133*, 43699.

KEYWORDS: blends; grafting; mechanical properties; polyurethanes; radical polymerization

Received 10 January 2016; accepted 26 March 2016
DOI: 10.1002/app.43699

INTRODUCTION

The graft copolymerization of polar monomers is a useful technique for the modification of the chemical and physical properties of polymer surfaces.[1,2] Graft copolymers have a number of important and unique advantages for use in applications involving the interfacing of synthetic materials and living systems.[3,4] By chemically bonding a polymer to the surface of another polymer, a new graft material is formed. The mechanical properties of this graft material can closely resemble those of the untreated substrate polymer, originally selected to have the appropriate modulus and durability for the intended application.[5] Moreover, for nonporous polymers that are free of diffusible low-molecular-weight components, biocompatibility is largely influenced by the surface properties of the polymer.[6] One particular method used to obtain functionalized polymers is grafting hydrophilic vinyl monomers onto hydrophobic backbones.[7]

Acrylic acid (AA) is a synthetic bio-stable monomer that is highly hydrophilic in nature, with many carboxylic side chains that enable conjugation with the functional groups of the substrate polymer.[8] Due to the ability to retain a significant portion of water, AA is considered an ideal choice for the modification of inherently-hydrophobic polymers such as styrene butadiene rubber (SBR).[9] This can efficiently address the low wettability (and therefore the low biocompatibility) of rubbers to ultimately produce a desired reaction in contact with a biological environment. Therefore, hydrophilic-modified polymers have found profound biomedical applications; in particular, as coatings for medical devices.[1,8] Many efforts have been made to investigate the effect of AA grafting on styrene-based (co)polymers.[10–17] Vesaratchanon *et al.* studied the formation of polymer brush layers in styrene butadiene latex particles copolymerized with acrylic acid and found that thick "hairy" layers were formed around the latex particles.[10] Acrylic acid

copolymerized latex was reportedly very sensitive to the pH and ionic strength, with acrylic acid layer expanding to 3–4 nm when the pH increased from 4 to 10. Yeganeh-Ghotbi and Haddadi-Asl explored the radiation grafting of two hydrophilic monomers (i.e., acrylamide and acrylic acid) onto SBR backbone and found that graft yields of acrylic acid grafted SBR (SBR-g-PAA) were higher than that of acrylamide, even though they both followed the same trends in regard with the monomer concentration.[11] They particularly focused on the morphology of the treated and untreated graft copolymers and observed that the untreated SBR sample had a smooth surface, while the surface of the grafted substrate became rougher, increasing progressively with the increase in the graft yields for both monomers. The graft yield was increased with concentration of acrylic acid according to Jiang and Wilkie and little difference was observed in the graft yield when benzoyl peroxide (BPO) and azobisisobutyronitrile (AIBN) were used as initiators.[12] They also reported that the AA monomers reacted with the double bond of the butadiene segment and formed heterogeneous reaction sites. Similar observations were reported in the graft copolymerization of acrylic acid on to acrylonitrile-butadiene-styrene (ABS) terpolymers (45 wt % styrene, 40 wt % butadiene, 15 wt % acrylonitrile).[13,14] Despite the evident importance of the mechanical characteristics of such copolymers for potential applications, very few studies have explored the mechanical properties of these grafted systems and the possible applicatory constraints that might be imposed upon grafting. Most relevant to the current research, Kennedy *et al.* studied the role of AA grafting on the mechanical and thermal properties of styrene butadiene styrene (SBS) graft copolymers (styrene/butadiene ratio ~45 wt %).[15] The grafting of acrylic acid monomer was reportedly occurred onto the butadiene segments of the SBS backbone and while the Young's modulus of the grafted sample was 2.7 times larger than the pure SBS (34 MPa compared to 14 MPa), a drastic reduction was observed in the deformability (and thus the toughness) of the grafted copolymers, which might hinder its implementation.

One feasible approach to overcome this issue is blending the grafted copolymers with a high-performance flexible polymeric matrix. Due to good physical strength, abrasion resistance, fatigue life, versatility and biocompatible character, polyurethane (PU) is widely used as a reinforcing polymeric system and is the material of choice here.[18] Nonetheless, PU and SBR does not possess close hydrophobic/hydrophilic balances and need major modifications in order to achieve compatibility. Taking the antecedents into account, the aim of the present study is to present interesting set of properties of a new acrylic acid-based SBR/PU blend, and controlling the end-product properties by tailoring phase morphology and the degree of compatibility. In the first stage, SBR-g-PAA (simply referred herein as SBR*) was synthesized using various AA concentrations. Subsequently, a series of SBR*/PU blends were prepared with 80:20, 70:30, and 60:40 phr of SBR* to PU. Acrylic acid is expected to have a dual effect here. First, it can act as a compatibilizer/interfacial agent for modifying immiscible polymer matrices, which are known for defects such as two-phase morphology, narrow interphase and poor physical and chemical interaction across the phase boundaries.[19] The compatibilizing effect of carboxylic acid groups has been pointed out for other immiscible polymeric blends such as polystyrene and polyamide, and can be considered as a paramount reference point in terms of feasibility of the current research.[20] Likewise, acrylic acid can introduce its hydrophilic character to the final polymer blend, which can make it an attractive material for potential bio applications.

EXPERIMENTAL

Materials

The styrene butadiene rubber (SBR) used in this study was Poliran SBR-1502, a low molecular weight (474.72 g mol^{-1}), unvulcanized, commercial polymer obtained from Iran Petrochemical Commercial Co (IPCC), with a density of 0.93 g cm^{-3} and a styrene content of ~22.5–24.5 wt %. Polyether-based polyurethane (PU) was synthesized using poly(tetrahydrofuran) (PTHF; M_n = 2000 g mol^{-1}), which was purchased from Sigma-Aldrich Chemie GmbH. The hard segments were synthesized from 1,6-hexamethylene diisocyanate (HDI) and 1,4-butanediol (BDO) obtained from Aldrich and Merck Chemicals, respectively. Acrylic acid monomer (AA; T_m = 13 °C) and benzoyl peroxide (BPO; linear formula $C_{14}H_{10}O_4$; M_w = 242.2 g mol^{-1}) were both purchased from Merck. Toluene and methanol (99.85% purity) were used as solvents and obtained from Sigma-Aldrich and Shiraz Petrochemical (Shiraz, Iran), respectively.

Synthesis of Grafted SBR* Copolymers via Free Radical Polymerization

SBR with no additional ingredients was initially dried at 80 °C for 6 h in a vacuum oven and then 2 g of the base polymer was dissolved in toluene (20 mL) at 60 °C. Benzoyl peroxide (3 wt % of the used SBR; 0.06 g) was added to the mixture as the initiator of the grafting process and allowed to be stirred in a rounded bottom three-neck reactor that was equipped with N_2 inlet, magnetic mixer and condenser for 15 min at 60 °C. Variable amounts of AA (50, 100, and 150 wt % of the used SBR; 1, 2, and 3 g, respectively) were then introduced to the reactor and stirred for another 6 h at speed of 600 rpm. The copolymerization reaction product was precipitated in cold methanol, washed three times with water, filtered and dried in a vacuum oven at 40 °C for 48 h. To remove non-grafted poly(acrylic acid) homopolymers and other residual chemicals, the reaction products were placed in a soxhlet extractor using methanol at 60 °C for 24 h. During this procedure, potential insoluble parts of the modified SBR was also extracted. This was an important step to make sure that the influence of gel fraction was eliminated for further analyses. The purified samples (SBR*) were placed in a fume cupboard for 24 h and then a vacuum oven at 60 °C for 6 h to be prepared for the blending procedure. The grafted SBR* copolymers are named indicating the AA concentration, as SBR*100 stands for a graft copolymer based on SBR matrix that was reacted with 100 wt % of acrylic acid.

Preparation of SBR*/PU Blends

A two-step *in situ* polymerization method was employed to synthesize polyurethane as reported elsewhere.[21] Briefly, a three-neck flask, equipped with nitrogen inlet and a mechanical stirrer system was used for the reaction of 1 mol poly(tetrahydrofuran) and 2.284 mol HDI (hard segment content = 20%). The chain extension reaction was then performed between 1 mol

Table I. Codes and Formulations of SBR Graft Copolymers and SBR/PU Blend Compositions

		Composition		
Sample	Code	SBR (phr[a])	AA (wt %[b])	PU (phr)
Neat SBR	SBR	100	0	0
Acrylic acid grafted SBR	SBR*050	100	50	0
Acrylic acid grafted SBR	SBR*100	100	100	0
Acrylic acid grafted SBR	SBR*150	100	150	0
Modified SBR/PU blend	SBR*100/PU 80:20	80	100	20
Modified SBR/PU blend	SBR*050/PU 70:30	70	50	30
Modified SBR/PU blend	SBR*100/PU 70:30	70	100	30
Modified SBR/PU blend	SBR*150/PU 70:30	70	150	30
Unmodified SBR/PU blend	SBR/PU 70:30	70	0	30
Modified SBR/PU blend	SBR*100/PU 60:40	60	100	40

[a] Part per hundred of resin.
[b] Weight percent that reacted with SBR prior to blending procedure.

prepolymer and 1 mol BDO. Before curing, the mixture was kept at 80 °C and 10 Pa in a vacuum chamber for 10 min to degas. The mixed materials were then heated for 48 h at 80 °C and then kept at the room temperature for a minimum of 30 days before subsequent using. The microstructure-property relationships of this PU system has been comprehensively analyzed in terms of parameters such as hard segment content, degree of phase separation, crystallinity of soft and hard domains, etc., and can be explored elsewhere.[21]

A series of SBR*/PU blends was prepared with 80:20, 70:30, and 60:40 phr of SBR* to PU (see Table I for the codes and formulations of different blend systems). Blends were prepared using a Barbender® internal mixer (Model Plasti-Corder PL 2200) at a speed of 100 rpm at 145 °C. Known amount of PU was initially introduced to the mixer and allowed to be completely grinded for 1 h. The unmodified SBR or SBR* was then added to the system and mixed with the PU particles for another 2 h. For DMTA and tensile testing, the specimens were placed in a 25 ton Davenport Laboratory compression molder at 145 °C for 10 min to obtain appropriate blend films.

Characterization

SBR* Graft Copolymers. To examine the completion of the grafting process, graft yield (GY) was calculated by the percentage increase in the mass as follows[22,23]:

$$\mathrm{GY}(\%) = \frac{m_g - m_0}{m_0} \times 100 \quad (1)$$

where m_0 and m_g represent the initial (2 g) and grafted masses of the SBR, respectively. Likewise, graft efficiency (GE) was measured by the percentage increase in the mass relative to the utilized AA[22,23]:

$$\mathrm{GE}(\%) = \frac{m_g - m_0}{m_{\mathrm{AA}}} \times 100 \quad (2)$$

where m_{AA} is the used amount of acrylic acid (1, 2, or 3 g) in the grafting procedure. To evaluate the grafting of AA monomers onto the SBR backbone, attenuated total reflectance infrared spectroscopy (ATR-IR) was carried out. The IR spectra of the neat SBR, AA and the grafted SBR*100 copolymer were acquired on a VERTEX 80 spectrometer (Bruker, Germany) with a signal resolution of 4 cm^{-1} within the 4000–600 cm^{-1} range. The number of scans was set at 16 for each sample. To further investigate the mechanism of the grafting process, dynamic mechanical thermal analysis (DMTA) was performed by a Tritec 2000 DMA (Triton Technology) device. The apparatus was carefully calibrated according to ASTM D7028 before each set of examination. DMTA thermograms of the neat and SBR* copolymers were obtained at a frequency of 1 Hz and heating rate of 4 °C/min from −100 to 120 °C.

SBR*/PU Blends. Scanning electron microscopy (SEM; Model Philips XL 30) was used to examine the surface morphology of the unmodified and modified SBR/PU blends. The scanning was performed at 15 kV while the surface of the specimens was coated with a thin gold layer (10 Å) prior to imaging to enhance the conductivity. WAXD measurements were carried out using a X'Pert PRO PANalytical diffractometer equipped with a Nickel-filtered Cu Kα radiation (λ = 1.5405 Å) with a tube voltage of 40 kV and tube current of 30 mA. The diffractograms were scanned at ambient temperature in the 2θ range from 0° to 40°, and with a step size of 0.03°. Dynamic-mechanical properties of blend compositions were evaluated using the same DMA device and under the same test conditions as the SBR* graft copolymers. Tensile tests were performed following ASTM D 412 type I method using a Zwick Z050 extensometer with a crosshead speed of 500 mm/min. Dumbbell type specimens for the tensile test were prepared using an appropriate punch. The values of various mechanical properties reported in this study represent averages of at least three samples. The aqueous swelling behavior was carried out in deionized water at 37 °C. The specimen in the form of rectangular films were first dried for 24 h under vacuum at 40 °C and weighed using a microbalance. They were subsequently immersed in deionized water, removed every 12 h, gently wiped off using a filter paper to remove the surface water, weighed, and immediately reimmersed in deionized water. Swelling measurements were conducted over a period of 10 days. The absorbed water content,

Table II. Effect of Monomer Concentration on the Graft Yields and Graft Efficiencies of SBR* Graft Copolymers

Graft copolymer code	Initial neat SBR (g)	Utilized AA monomer (g)	GY[a] (%)	GE[b] (%)
SBR*050	2	1	21.1	42.2
SBR*100	2	2	43.6	43.6
SBR*150	2	3	37.1	24.7

[a] Graft yield.
[b] Graft efficiency.

expressed as water absorption ratio (%), was determined from the relative weight gain of the samples by:

$$\text{Water absorption ratio (\%)} = \frac{w_t - w_0}{w_0} \times 100 \qquad (3)$$

where w_t is the weight of the sample at time t and w_0 is the initial weight of the specimen.

RESULTS AND DISCUSSION

Synthesis and Characterization of SBR* Graft Copolymers

Graft Yield (GY) and Graft Efficiency (GE). The effect of monomer concentration on the graft yield of the SBR* copolymers is investigated and the results are presented in Table II. The GY increased with increasing monomer concentration up to 100 wt %. This is an expected behavior, since the greater the concentration of monomer, the more macroradicals will form and the more opportunity there will be for reaction of a macroradical with SBR substrate. Increasing trend of monomer concentration, however, led to a meaningful reduction in the value of the graft yield. This can be attributed to the increase in the viscosity of the medium due to the increase in the monomer concentration (and thus the increasing possibility of homopolymerization). The elevation in the viscosity hindered the movement of the monomers toward the substrate and consequently reduced the graft yield.[24] Likewise, the intermolecular chain-transfer reaction increased with monomer concentration, which led to further homopolymerization. Due to the dependence of GY on the amount of the utilized AA, graft efficiency might give a better vision of the grafting nature. As seen in Table II, SBR*100 had a graft efficiency of 43.6%, meaning that 56.4% of the AA monomers were washed away as homopolymers or unreacted monomers. At 150 wt % of AA concentration, a value of 24.7% was recorded for GE due to the progressive rate of homopolymerization.

ATR-IR Spectroscopy. The ATR-IR spectra of the neat SBR, AA and SBR*100 are illustrated in Figure 1. The spectrum of the neat SBR showed (a) characteristic bands corresponding to the butadiene segments at 964 cm^{-1} (trans-1,4),[25] 1638 cm^{-1} (stretching vibration of vinyl),[26] 1450 cm^{-1} (—CH_2 scissoring), 3026 cm^{-1} (=CH stretching),[27] 2844 and 2916 cm^{-1} (C—H stretching).[21] Likewise, vibrations at 698 cm^{-1} (styrene units), 1602 cm^{-1} (aromatic C—C stretching) and 3066 cm^{-1} (C—H out of plane deformation) were observed for the styrene segments of the neat SBR.[15,19] In terms of acrylic acid, the most prominent bands were the sharp carbonyl vibration at 1718 cm^{-1},[28] and the very broad —OH stretching band at 3147 cm^{-1} (b).[25,29] Furthermore, the bands at 1405 and 1180 cm^{-1} were due to the COH inplane deformation and C—O stretching vibrations within the AA structure.[30] As can be seen in Figure 1(c), the IR spectrum of the grafted SBR*100 copolymer revealed a new absorption band (compared to its neat SBR counterpart) at 1736 cm^{-1}, which is related to the stretching vibration of the free carbonyl groups. Botros *et al.*[19] also found this peak in SBR-g-PAA at 1728 cm^{-1} whilst Kennedy *et al.* located this peak at 1725 cm^{-1} on grafted styrene butadiene styrene-g-acrylic acid (SBS-g-AA) copolymers.[15] The presence of this new band suggests that the grafting of acrylic acid on the SBR chains is successfully achieved. Note that the styrene vibration at 698 cm^{-1} diminished in the grafted sample relative to its equivalent band in the pure SBR. This is taken to mean that grafting of the monomers was possibly occurred onto the styrene segments of the SBR backbone.

Although IR spectroscopy is a widely-used method to confirm that grafting has taken place, it does not give detailed information in regard with the reaction sites and the possible mechanism of the grafting process. Therefore, a much more sensitive characterization method such as dynamic mechanical thermal analysis (DMTA) could be of particular interest here.

Dynamic Mechanical Thermal Analysis (DMTA). tan δ and storage modulus thermograms of the neat SBR and the grafted SBR* copolymers that obtained from the DMTA experiments, are shown in Figure 2. The glass transition temperature (T_g) is determined as the peak of the tan δ plot (tan $\delta = G''/G'$; G'' and G' are the loss and storage modulus, respectively). Two tan δ peaks, the low glass transition temperature (T_{g1}) associated

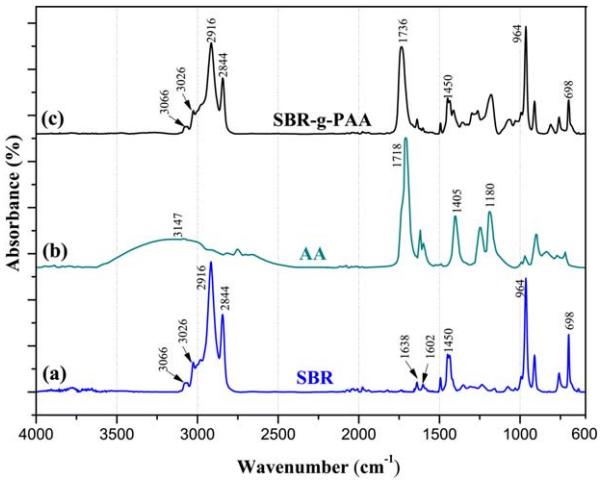

Figure 1. ATR-IR spectra of (a) pure SBR, (b) acrylic acid, and (c) SBR*100. [Color figure can be viewed in the online issue, which is available at wileyonlinelibrary.com.]

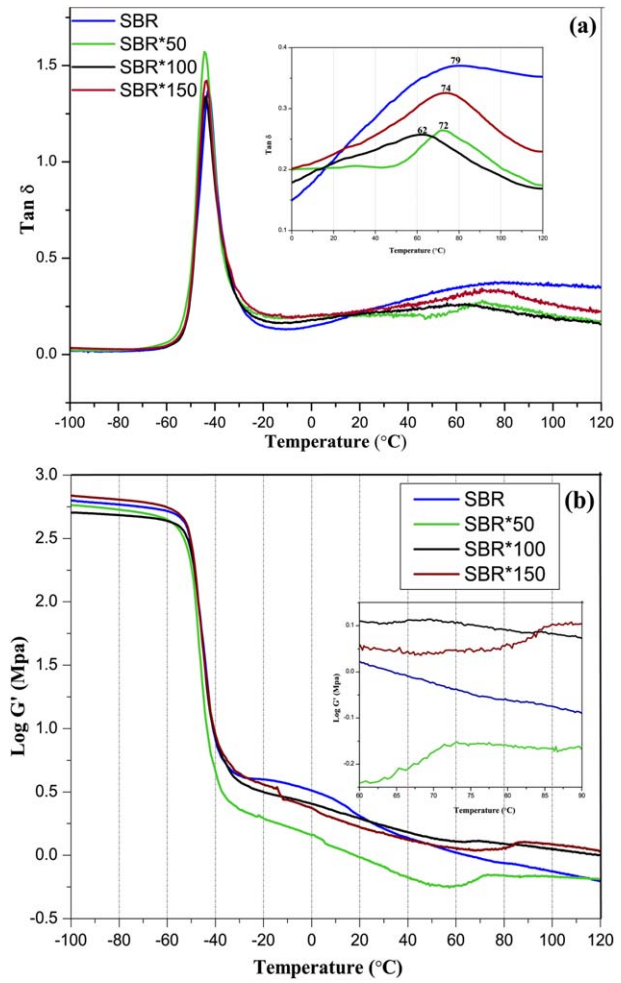

Figure 2. DMTA results of the neat SBR and SBR* graft copolymers modified with various AA concentrations: (a) tan δ vs. temperature plot (the magnified insert associated with the glass transition of styrene segments is included for better clarity); (b) storage modulus–temperature plot in logarithmic scale. [Color figure can be viewed in the online issue, which is available at wileyonlinelibrary.com.]

with the butadiene segments (~−44 °C) and the high glass transition temperature (T_{g2}) of the styrene domains (~79 °C), were observed for the neat SBR and the grafted SBR* copolymers. Therefore, the overall microphase-separated structure of the soft butadiene chains and the hard styrene domains within the SBR system is maintained for the graft copolymers. As illustrated in Figure 2(a), the values of T_{g1} were almost constant for all of the samples, while the T_{g2} values reduced upon grafting [see the magnified inset in Figure 2(a)]. Thus, it can be confirmed that the grafting of AA occurred onto the styrene segments along the SBR backbone. This is due to the fact that throughout the grafting process, the high concentration butadiene rubbers (~75.5–77.5 wt %) were well-dissolved in the solvent because of their low glass transition temperature, while styrene segments could partially maintain their dimensional stability. Therefore, the modifying monomer preferably attached to the segments with the least macromolecular motion.[31] Kennedy *et al.*[15] and Chandrasiri *et al.*[12] reported grafting of acrylic acid onto the poly(butadiene) segments of SBS and ABS co/terpolymers, respectively. However, in both cases the styrene content was as high as 45 wt %, with the total molecular weight (M_w) of 102,000 g mol^{-1} for SBS and 280,000 g mol^{-1} for ABS. This is respectively 214 and 589 times higher M_w compared to the employed SBR in this report. Thus, because of the high-level of energy that was required for the production of free radicals in styrene segments, the separation of hydrogen atoms was hardly accomplished in the aforementioned reports, which in turn can be ascribed to the shielding effect of aryl groups in styrene-butadiene backbone.[11] Furthermore, when the styrene segment is sufficiently high, crosslinking of poly(styrene) segments reportedly occurs, which drastically decreases the feasibility of acrylic acid grafting.[32] On the other hand, Ning *et al.*[32] synthesized block-graft copolymers of [poly(styrene-*b*-ethylene-*co*-butylene-*b*-styrene)-*g*-poly(acrylic acid)] with the styrene content of 28.6 wt %, and observed that the grafts were attached to the poly(styrene) end blocks. de la Fuente *et al.*[33] reported the graft copolymerization of poly(acrylic acid-*g*-styrene) via a facile hydrolysis method, with the FTIR spectra of the final graft copolymer being in outstanding adjacency the SBR*100 sample presented in this work. Therefore, the styrene content and the molecular weight of styrene butadiene-based (co)polymers are important factors in determining the site of the grafting reaction. A proposed scheme of the reaction between SBR and AA to attain SBR* graft copolymers is depicted in Figure 3. The acrylic acid monomers were supposedly reacted with the allylic hydrogen atoms associated with the styrene segments within the SBR chains.

In terms of macromolecular motion capacity of chain segments, two counteracting effects were observed in the tan δ curves of the grafted SBR*; the decrease of the glass transition temperature (T_{g2}) and the reduction of T_{g2} peak height values. T_g correlates well with the interfacial energy between the polymer matrix and the grafted modifier and therefore, the reduction of the T_{g2} values in the SBR* copolymers can be interpreted as the

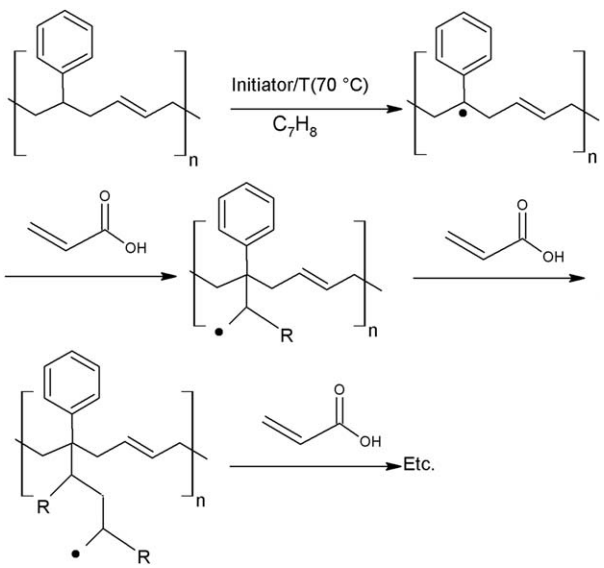

Figure 3. Schematics of the grafting reaction to obtain SBR* graft copolymers.

increased macromolecular motion capacity (lower interfacial energy) due to the grafting that has occurred. On the other hand, the height of the glass transition peak in a tan δ vs. temperature thermogram has been frequently linked to the number of kinetic units within the chain segments, which are mobile enough to contribute to the glass transition.[15,34] Based on the height of the tan δ plot in Figure 2(a), the mobility of the kinetic units is reduced in the grafted copolymers due to the grafting which took place. The result of the simultaneous occurrence of such effects is expected to be the maintenance of the flexible character of the SBR* as opposed to previous reports, where the reduction of tan δ peak height has occurred in conjunction with an increase of the T_g values, leading to flexibility constraints.[15,35,36] The values of storage modulus at $T = -100\,^{\circ}C$ [Figure 2(b)] further clarified that grafting of AA up to 100 wt % led to a more viscoelastic behavior (lower G' in logarithmic scale), while at 150 wt % of AA concentration an uprise in log G' value was observed, which showed that an "optimum" AA concentration exists in regard with sustaining the deformable nature of the rubber. Furthermore, it demonstrated that molecular mobility of graft copolymers increase with an increase in GY as reported elsewhere.[37] As shown by the magnified inset in Figure 2(b), the values of log G' continuously decreased for the pure SBR, while SBR* samples showed slight increases of the storage modulus (in a five-celsius interval for each sample), continued by the usual, characteristic reduction thereafter. The temperature range in which this phenomenon occurs is related to the transition temperatures of the styrene segments. Likewise, it is known that acrylic acid toughens the polymer substrate that it has grafted onto.[8,15,19] Hence, this partial increment of the storage modulus values can be ascribed to the toughening effect of acrylic acid monomers that have grafted on to the styrene segments of the SBR backbone.

Properties of SBR*/Polyurethane Blends

Morphology of SBR*/PU Blends. In order to evaluate the influence of AA concentration on the miscibility of SBR*/PU blends, SEM micrographs are taken, as illustrated in Figure 4(a–f). The concentration ratio of SBR to PU was fixed at 70:30. Two different phases, the dark base polymer associated with the SBR* and the PU chains in the form of white bright particles, appeared in the micrographs. As depicted in Figure 4(a), the unmodified SBR was largely incompatible with PU and PU aggregates in the size of 10 μm were formed. This was due to the high interfacial tension and polarity differences between the two immiscible polymer systems, which resulted in a weak interface and poor dispersion state. SBR*050/PU showed [Figure 4(b)] well-dispersed PU particles in the SBR matrix with occasional aggregates [marked in Figure 4(b) by an arrow], which were significantly smaller in size compared to the unmodified SBR/PU blend. At higher magnifications, the most prominent feature of the surface was revealed [Figure 4(c)] to be a granular structure consisting of small, uniform PU particles, which were up to 500 nm in size. As discussed in DMTA analysis, lower glass transition temperature was achieved for the graft copolymers compared to their untreated SBR counterpart, which led to lower interfacial energies (higher interfacial adhesions) and ultimately improved miscibility of the modified blends. SBR*100/PU revealed [Figure 4(d)] one-phase morphology with no macro-scale phase separation between the two polymer constituents, indicating a remarkable enhancement in the homogeneity of the sample. As clearly seen from Figure 4(d,e) the interconnected surface morphology of the SBR*100/PU 70:30 sample became severely rougher compared to other specimens, which was an anticipated phenomenon as reported by Yeganeh-Ghotbi and Haddadi-Asl.[11] However, by further increase of the AA concentration in the grafting process, the resulting PU blend (SBR*150/PU) did not show any improvement in regard with the size and distribution level of the PU particles. As illustrated in Figure 4(f), the surface structure of the SBR*150/PU sample was distributed with intermittent, stretched out PU particles in the range of 0.3–3 μm in size. The "optimum" blend system with regard to the homogeneity of the polymer components was achieved at 100 wt % concentration of AA and is considered to be the ideal candidate in controlling the degree of compatibility of blend compositions. These observations can also be expressed in regard with the positive correlation between the GY of SBR* copolymers and the level of compatibility of the resultant blend system, as SBR*100 with the highest GY proved to be the best compatible component for PU blend. The following part will mainly discuss the influence of SBR*100 to PU ratio on the physical properties of SBR*100/PU blends.

Wide-Angle X-ray Diffraction (WAXD) Analysis. In order to confirm the formation structure of SBR*100/PU blends, WAXD was carried out ($2\theta = 0°$–$40°$) and the results are depicted in Figure 5. A broad amorphous halo was observed for SBR*100 at a diffraction scattering angle of 20°, which is characteristic of inherently amorphous rubber matrices such as SBR.[38] Pristine PU exhibited an apparent amorphous halo in the same 2θ region. Nonetheless, a previous study on the influence of hard segment content (HSC) on the crystallinity of PTHF-based polyurethanes revealed that in fact three sharp reflections exist in the 2θ range of 20°–24°, which gradually become evident as HSC increases.[21] The first two reflections at 19.8° and 21.5° are obscure in Figure 5 because of their strong juxtaposition. The PU's 23.5° reflection, however, is prominent in the diffractogram and is related to the lateral distances at the interfaces of the hard crystallized segments. All blend compositions showed the characteristic reflection at $2\theta = 23.9°$, indicating that the partial crystallinity of PUs was integrated to the final blend products. Note that at 60:40 ratio of SBR*100 to PU, the 23.9° reflection was at its most intensified state among all blend compositions, which showed that the formation of semicrystalline structure in blend compositions had a positive correlation with PU content. Furthermore, the reflection position revealed that all blend samples shifted slightly toward higher angles (smaller d values), which can be explained by the increase of compactness and densification of polymer chains during the blending procedure.

Dynamic-Mechanical Properties of Blend Compositions. The influence of PU incorporation on the storage modulus in logarithmic scale (G') and damping factor (tan δ) of the grafted SBR* is illustrated in Figure 6(a,b). As previously discussed, the peak of tan δ vs. temperature—which is taken as the value of glass transition temperature—appeared at $\sim -44.5\,^{\circ}C$ for

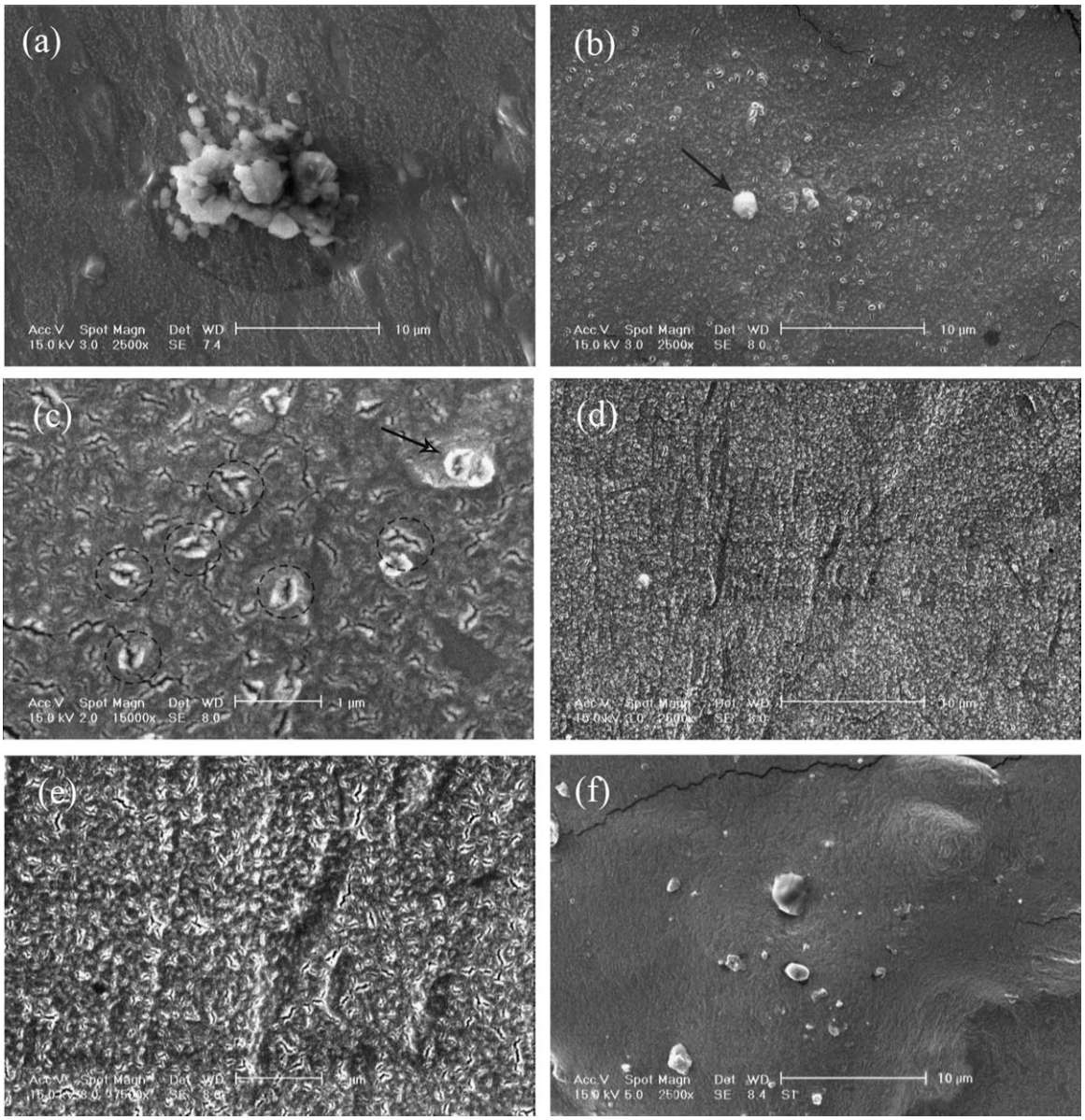

Figure 4. SEM micrographs of 70:30 blends at the magnification of 10 μm for (a) unmodified blend, and blend samples that were modified with (b) 50 wt % (SBR*050/PU 70:30); (d) 100 wt % (SBR*100/PU 70:30) and (f) 150 wt % of AA (SBR*150/PU 70:30). Higher magnification images at 1 μm and 2 μm are shown for (c) SBR*050/PU 70:30, and (e) SBR*100/PU 70:30, respectively.

SBR*100. Pristine PU exhibited a relatively broad peak at −59.6 °C, which is ascribed to the glass transition of poly(tetrahydrofuran) soft segments.[39] All blend compositions showed one distinctive tan δ peak at the approximate temperature of the average T_g of PU and SBR*100 (∼−51.3 °C). The appearance of only one altered, distinctive glass transition is a conspicuous manifestation of homogeneous miscibility of the two polymer components. As many end-product properties are "T_g-related", the achievement of a single T_g in compatible blends is of particular interest in many engineering applications, and contrasts sharply with two or more T_g values in incompatible blends.[40] The reinforced blends exhibited a progressive reduction in tan δ peak height to compensate for an increase in storage modulus [Figure 6(a)]. With the increase in PU loading, the tan δ diagrams are shifted downwards, indicating a less energy-dissipative behavior for blends in comparison with the grafted SBR*100.

Pristine PU had an outstanding storage modulus in the order of 2 GPa in glassy state. As reported by Sonnenschein *et al.* semicrystalline soft segment in PU leads to significant modulus increase since the crystals act as reinforcements, in addition to the hard domains.[41] Figure 6(b) illustrates that the aforementioned reinforcing effect was introduced to all blend compositions as the value of log G' consistently improved both below and above the glass transition compared to SBR*100. The initial slope of the thermogram at −100 °C increased with PU loading to continuously resemble that of the pristine PU, indicating that

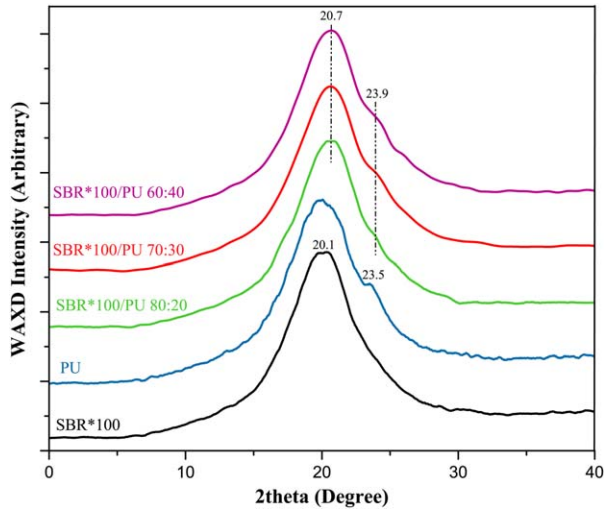

Figure 5. Wide-angle X-ray diffraction of SBR*/PU blends and their raw constituents. [Color figure can be viewed in the online issue, which is available at wileyonlinelibrary.com.]

the unique characteristics of both of the polymer components were integrated to the final blend samples. Likewise, the blends developed a stable rubbery plateau region at elevated temperatures up to 100 °C due to the dimensional stability of the rigid PU hard domains that served as physical crosslinks in the rubber matrix.

Tensile Properties. The mechanical properties of blend compositions were investigated by the tensile testing in SBR/PU ratios of 80:20, 70:30, and 60:40. The typical stress–strain curves of the blends and their raw constituents are illustrated in Figure 7(a) and the characteristic values of the tensile modulus, toughness, stress, and strain at break are summarized in Table III. The tensile modulus was determined by taking the slope of stress–strain curve at linear low-strain range (1–5%). Upon grafting of pure SBR with 100 wt % of acrylic acid, the tensile modulus increased with a minimal compensation on elongation at break. This is well-consistent with literature and is a result of grafting AA on to the SBR backbone, which has reduced the flexibility (albeit small) thus making the material stiffer.[15,35,36] This issue was addressed by the effective mixing of PU with the grafted copolymer. All the blend systems exhibited a linear elastic behavior at low stress region and plastic deformation at high stress region. The tensile strength and modulus, elongation at break, and toughness of blend compositions are synchronously improved in comparison with the modified SBR*100, which is very unusual in polymer blends.[42] This is due to the strain-induced crystallization (SIC) of the high-concentration soft segments (SS) of PU. As a general trend, Figure 7(a) reflects that the increase of PU ratio leads to a progressive upturn in the slope of strain-hardening region ($\varepsilon > 100\%$). This upturn which is attributed to the strain-induced crystallinity of SS is the key factor for the simultaneous improvement of the tensile strength, modulus, and toughness. The SIC as well as the interfacial bonding between SBR network and PU particles can be revealed by plotting the reduced stress σ^* versus the reciprocal of the extension ratio α (ratio of the final length of the sample in the direction of stretch to the initial length before deformation), as suggested by the empirical Mooney–Rivlin equation[43]:

$$\sigma* = \frac{\sigma}{2(\alpha - \alpha^{-2})} = C_1 + C_2\alpha^{-1} \quad (4)$$

where C_1 and C_2 are constants, independent of α which are ascribed to the network structure and the flexibility of the network, respectively.[44] A predominant linear region was observed for the neat SBR and SBR*/PU blend compositions with a sharp decline of σ^* in the region of small extension ratio ($\alpha^{-1} > 0.8$), which can be ascribed to Payne effect.[45] Pristine PU showed SIC characterized by an abrupt upturn behavior in the region of large extension ratio ($\alpha^{-1} < 0.4$). This is often observed when a highly uniform microstructure of polymer chains exists, and is responsible for the large and steep increase in the reduced stress in the adjacency of the maximum deformation (low α^{-1}).[43,46] Oriented crystallites act as surplus crosslinking points, and to some extent as filler particles that give rise to immense improvement of the strength and fatigue properties of the

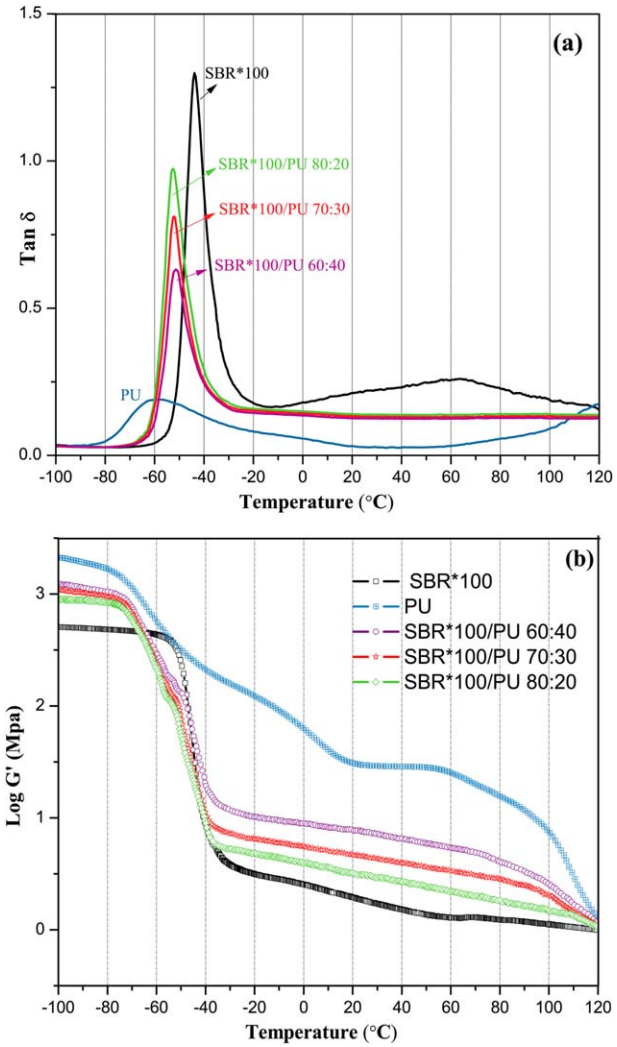

Figure 6. DMTA results of SBR*100, pure PU, and SBR*/PU blends at various ratios: (a) tan δ vs. temperature plot; (b) storage modulus–temperature plot in logarithmic scale. [Color figure can be viewed in the online issue, which is available at wileyonlinelibrary.com.]

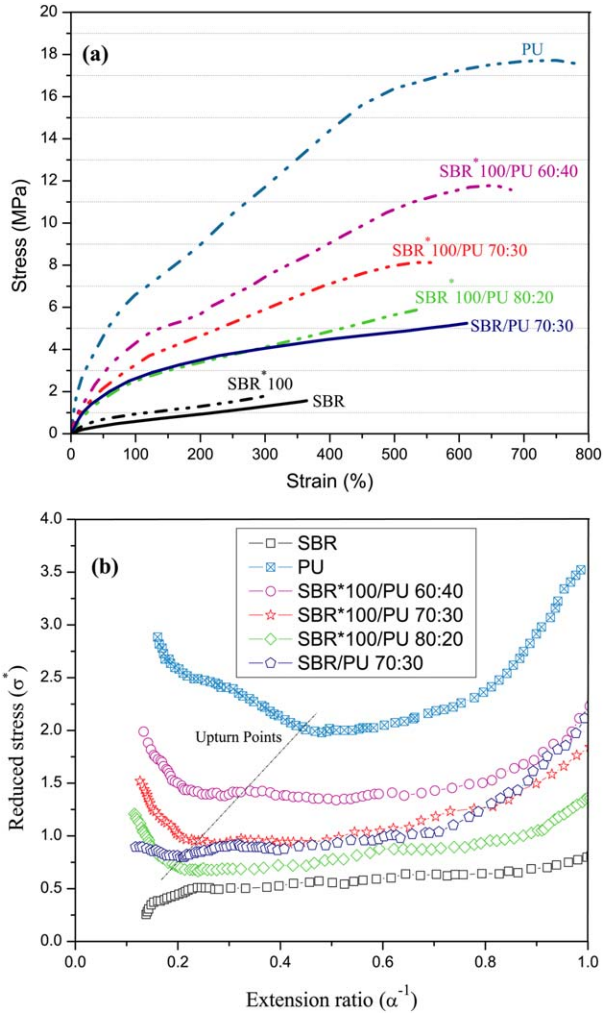

Figure 7. Mechanical properties of the neat PU, neat SBR, SBR*100, the unmodified 70:30 blend system, and SBR*/PU blends at different ratios: (a) typical stress–strain curves and (b) Mooney–Rivlin plots. [Color figure can be viewed in the online issue, which is available at wileyonlinelibrary.com.]

elastomer. From Figure 7(b), it can be observed that the upturn behavior was persistent in all the modified SBR*/PU blend compositions despite the fact that the neat SBR did not undergo SIC, and exhibited a decreased σ^* attributed to the affine-phantom transition at $\alpha^{-1} < 0.25$.[40] The upturn behavior in the presence of a reinforcing agent is due to the finite extensibility of polymer chains bridging neighboring polymer component and is observed when a strong interfacial bonding between the two polymer components exists. The upturn points shifted to lower extension ratio with the increase of PU content, indicating that the self-toughening behavior of blend compositions can be initiated at lower deformations with PU loading. It might be noteworthy to mention that SIC is closely related to the regularity of packing of the polyurethane's soft segments. Likewise, mechanical properties such as resilience is to a great extent influenced by the compatibility of rubber blend components,[40] which additionally indicates that PU chain segments have a high degree of orientation within SBR*100 matrix. Moreover, the modified interface (as revealed by SEM analysis) played a pivotal role in reinforcing the SBR*100 matrix by effectively transferring stress between the SBR*100 and the more durable PU system, so as by introduction of only 20 phr of polyurethane (SBR*100/PU 80:20), the values of tensile modulus, elongation at break, toughness, and maximum stress improved by 190, 77, 506, and 221%, respectively.

In order to assess the extent of AA modification on the mechanical performance of the blend compositions, the stress-strain diagram of the unmodified SBR/PU 70:30—whose two-phase, incompatible morphology was depicted in Figure 4(a)—was also included. SBR*100/PU 70:30 showed 30, 55, and 11.5% improvement compared to its unmodified counterpart for the values of toughness, tensile strength, and the Young's modulus, respectively. This is due to the fact that a localization of shear stress [as revealed by the absence of upturn behavior in Figure 7(b) for SBR/PU 70:30] can occur at the narrow interface of the unmodified blend, giving rise to relatively poor tensile properties.

Swelling Behavior. The grafting of hydrophilic monomers such as acrylic acid has been found to increase the wettability of the grafted polymers.[18,47,48] Apart from the ability to retain a significant fraction of water within its structure, hydrophilic grafted polymers have extensive applications in biomedical application.[47–51] Thus, it is essential to investigate the water absorption properties of the blend systems to see if the proposed wettability has been introduced to the final blend compositions.

The effect of AA modifier, PU ratio, and the immersion time on the water absorption ratio of the SBR*/PU blends is illustrated in Figure 8. The pure SBR showed an extremely slow response to swelling, and absorbed approximately 4% of water after 4 days.

Table III. Tensile Properties of SBR/PU Blends and their Raw Constituents with Corresponding Standard Deviations

Sample code	Tensile modulus (MPa)	Tensile strength (MPa)	Elongation at break (%)	Toughness (Mj m^{-3})
SBR	1.3 ± 0.08	1.6 ± 0.04	364 ± 13	3.14 ± 0.15
SBR*100	2.8 ± 0.06	1.8 ± 0.09	305 ± 13	3.37 ± 0.17
PU	25.9 ± 0.66	17.6 ± 0.78	785 ± 21	99.51 ± 3.65
SBR*100/PU 80:20	8.2 ± 0.28	5.9 ± 0.28	541 ± 18	20.36 ± 1.32
SBR*100/PU 70:30	10.8 ± 0.33	8.1 ± 0.54	556 ± 20	29.95 ± 1.77
SBR/PU 70:30	9.7 ± 0.12	5.2 ± 0.11	612 ± 23	23.12 ± 1.45
SBR*100/PU 60:40	12.2 ± 0.27	11.8 ± 0.31	680 ± 32	52.96 ± 2.17

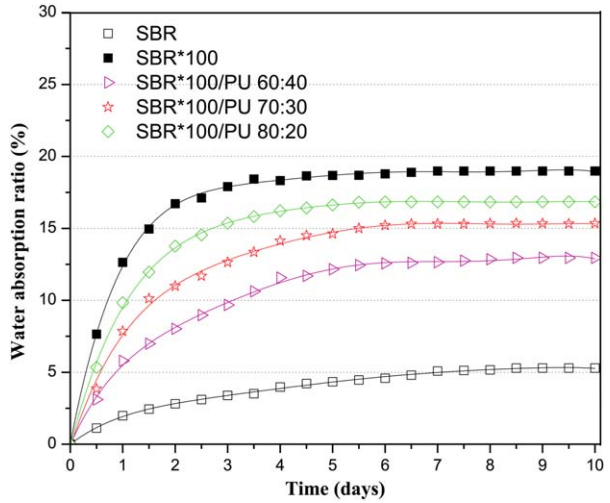

Figure 8. Water absorption behavior of the neat SBR, SBR*100 graft copolymer, and SBR*/PU blends in deionized water at 37 °C as a function of immersion time. [Color figure can be viewed in the online issue, which is available at wileyonlinelibrary.com.]

This was due to the hydrophobic nature of the rubber matrix. The water absorption ratio of the neat SBR leveled off (~5%) at the day 8 of the immersion, with infrequent variations observed thereafter. Upon grafting of 100 wt % of AA, the rate of water uptake increased dramatically, which is indicative of water-responsive materials. Likewise, the equilibrium water absorption ratio promoted to 19% (within 6 days of the immersion time) in the SBR*100 graft copolymer, showing a 258% water uptake increase in comparison with the neat SBR. This is ascribed to the hydrophilic nature of the AA chains that elevated the diffusion of water within the hydrophobic SBR matrix. Likewise, all the blend compositions showed improved swelling behavior compared to the neat SBR, verifying that the hydrophilic characteristic of AA was introduced to the blend samples as well. Nevertheless, the water uptake behavior of blend samples was restricted with PU loading due to the crystallinity of soft segments, as well as the crosslinking density of the used polyurethane.

CONCLUSIONS

In order to modify the incompatible nature of immiscible polymers, i.e., SBR and PU, acrylic acid was grafted onto the SBR backbone. The simultaneous reduction of tan δ peak heights and values corresponding to the styrene segments of the modified SBR, confirmed the grafting site. This was due to the low molecular weight of the unvulcanized SBR, as well as the relatively low styrene content, which led to the formation of styrene-grafted sites without any use of high-energy initiation methods such as photoinitiation. The morphology of the resultant polymer blends conspicuously showed the compatibilizing effect of acrylic acid. A gradual improvement of miscibility between the blend components was revealed with monomer concentration. At 100 wt % of AA concentration, in particular, a granular, interconnected structure was observed for the surface morphology that was characteristically rougher in comparison with the untreated blend sample. All blend compositions showed one distinctive tan δ peak at the estimated temperature of the average T_g of PU and SBR*100, which further verified that the modified blend constituents were miscible. Moreover, the semi-crystalline structure of PU was successfully integrated into the grafted rubber matrix as indicated by the appearance of the strain-hardening region in the stress-strain curves of the modified blends. The grafted copolymers also introduced improved wettability to the final polymer blends, owing to the hydrophilic nature of the acrylic acid monomers.

REFERENCES

1. Gupta, K. C.; Sahoo, S. *Biomacromolecules* **2001**, *2*, 239.
2. Li, M.-C.; Lee, J. K.; Cho, U. R. *J. Appl. Polym. Sci.* **2011**, *125*, 405.
3. Wang, D.; Xu, W.; Sun, G.; Chiou, B. *ACS Appl. Mater. Interface* **2011**, *3*, 2838.
4. Li, M.-C.; Cho, U. R. *Mater. Lett.* **2013**, *92*, 132.
5. Ratner, B. D. *J. Biomed. Mater. Res.* **1980**, *14*, 665.
6. Thevenot, P.; Hu, W.; Tang, L. *Curr. Top. Med. Chem.* **2008**, *8*, 270.
7. Garcia, A.; Berthelot, T.; Viel, P.; Mesnage, A.; Jegou, P.; Nekelson, F.; Roussel, S.; Palacin, S. *ACS Appl. Mater. Interfaces* **2010**, *2*, 1177.
8. Duan, L. J.; Liu, Y.; Kim, J.; Chung, D. J. *J. Appl. Polym. Sci.* **2013**, *130*, 131.
9. Weibel, D. E.; Vilani, C.; Habert, A. C.; Achete, C. A. *J. Membr. Sci.* **2007**, *293*, 124.
10. Vesaratchanon, J. S.; Takamura, K.; Willenbacher, N. *J. Colloid Interface Sci.* **2010**, *345*, 214.
11. Yeganeh-Ghotbi, M.; Haddadi-Asl, V. *Iran. Polym. J.* **1999**, *9*, 183.
12. Jiang, D. D.; Wilkie, C. A. *Eur. Polym. J.* **1998**, *34*, 997.
13. Chandrasiri, J. A.; Wilkie, C. A. *J. Polym. Sci. A: Polym. Chem.* **1996**, *34*, 1113.
14. Deacon, C.; Wilkie, C. A. *Eur. Polym. J.* **1996**, *32*, 451.
15. Kennedy, J. E.; Lyons, J. G.; Geever, L. M.; Higginbotham, C. L. *Mater. Sci. Eng. C* **2009**, *29*, 1655.
16. Bendejacq, D.; Ponsinet, V.; Joanicot, M. *Macromolecules* **2002**, *35*, 6645.
17. Mahdavian, A. -R.; Abdollahi, M. *Polymer* **2004**, *45*, 3233.
18. Yang, J.-M.; Huang, M. J.; Yeh, T.-S. *J. Biomed. Mater. Res.* **1999**, *45*, 133.
19. Botros, S. H.; Tawfik, S. Y. *Polym. Plast. Technol.* **2006**, *45*, 829.
20. Zhang, L.; Brostowitz, N. R.; Cavicchi, K. A.; Weiss, R. A. *Macromol. React. Eng.* **2014**, *8*, 81.
21. Taheri, S.; Sadeghi, G. M. M. *Appl. Clay Sci.* **2015**, *114*, 430.
22. Deng, F.; Ge, X.; Zhang, Y.; Li, M.-C.; Cho, U. R. *J. Appl. Polym. Sci.* **2015**, *132*, DOI: 10.1002/app42666.
23. Deng, F.; Zhang, Y.; Li, M.-C.; Li, X.; Cho, U. R. *J. Appl. Polym. Sci.* **2016**, *133*, DOI: 10.1002/app43087.
24. Kattan, M.; El-Nesr, E. *J. Appl. Polym. Sci.* **2006**, *102*, 198.
25. Liu, M.; Peng, Q.; Luo, B.; Zhou, C. *Eur. Polym. J.* **2015**, *68*, 190.

26. Bai, J.; Shi, Z.; Yin, J.; Tian, M. *Macromolecules* **2014**, *47*, 2964.
27. Hirayama, D.; Saron, C. *Indus. Eng. Chem. Res.* **2012**, *51*, 3975.
28. Beltrán, A.; Gómez-Emeterio, B. P.; Marco, C.; Ellis, G.; Parellada, M. D.; Díaz-Requejo, M. M.; Corona-Galván, S.; Pérez, P. J. *Macromolecules* **2012**, *45*, 9267.
29. Jung, W.-H.; Choi, Y.-S.; Moon, J.-M.; Tortorella, N.; Beatty, C. L.; Lee, J.-O. *Environ. Sci. Technol.* **2009**, *43*, 2563.
30. Sarkar, A. K.; Pal, A.; Ghorai, S.; Mandre, N. R.; Pal, S. *Carbohydr. Polym.* **2014**, *111*, 108.
31. Haque, H. A.; Nagano, S.; Seki, T. *Macromolecules* **2012**, *45*, 6095.
32. Ning, F.; Jiang, M.; Mu, M.; Duan, H.; Xie, J. *J. Polym. Sci. A: Polym. Chem.* **2002**, *40*, 1253.
33. de la Fuente, J. L.; Wilhelm, M.; Spiess, H. W.; Madruga, E. L.; Fernández-Garcia, M.; Cerrada, M. L. *Polymer* **2005**, *46*, 4544.
34. Mateo, J. L.; Bosch, P.; Serrano, J.; Calvo, M. *Eur. Polym. J.* **2000**, *36*, 1903.
35. Xu, Y.; Fang, Z.; Tong, L. *J. Appl. Polym. Sci.* **2005**, *96*, 2429.
36. Liu, Y.; Lv, C.; Yang, J. In Advances in Computer Science and Engineering; Zeng, D., Ed.; Springer: New York, **2012**; AISC *141*, p 335.
37. Chen, Z.; Fang, P.; Wang, H.; Wang, S. *J. Appl. Polym. Sci.* **2008**, *107*, 985.
38. Ozbas, B.; Toki, S.; Hsiao, B. S.; Chu, B.; Register, R. A.; Aksay, I. A.; Prud'homme, R. K.; Adamson, D. H. *J. Polym. Sci. B: Polym. Phys.* **2012**, *50*, 718.
39. Rueda-Larraz, L.; d'Arlas, B. F.; Tercjak, A.; Ribes, A.; Mondragon, I.; Eceiza, A. *Eur. Polym. J.* **2009**, *45*, 2096.
40. Wetton, R. E.; Corish, P. *J. Polym. Test.* **1989**, *8*, 303.
41. Sonnenschein, M. F.; Lysenko, Z.; Brune, D. A.; Wendt, B. L.; Schrock, A. K. *Polymer* **2005**, *46*, 10158.
42. Tahir, M.; Stöckelhuber, K. W.; Mahmood, N.; Komber, H.; Formanek, P.; Wießner, S.; Heinrich, G. *Eur. Polym. J.* **2015**, *73*, 75.
43. Joly, S.; Garnaud, G.; Ollitrault, R.; Bokobza, L. *Chem. Mater.* **2002**, *14*, 4202.
44. Rooj, S.; Das, A.; Heinrich, G. *Eur. Polym. J.* **2011**, *47*, 1746.
45. Li, M.-C.; Zhang, Y.; Cho, U. R. *Mater. Des.* **2014**, *63*, 565.
46. Lin, T.; Zhu, L.; Chen, W.; Wu, S.; Guo, B.; Jia, D. *Appl. Surf. Sci.* **2013**, *280*, 880.
47. Bhattacharya, A.; Rawlins, J. W.; Ray, P. Polymer Grafting and Crosslinking; Wiley: Hoboken, New Jersey, **2009**, pp 125–142.
48. Wang, X.; Chen, J.; Hong, K.; Mays, J. W. *ACS Macro Lett.* **2012**, *1*, 743.
49. Li, M. -C.; Ge, X.; Cho, U. R. *Macromol. Res.* **2013**, *21*, 793.
50. Halacheva, S. S.; Adlam, D. J.; Hendow, E. K.; Freemont, T. J.; Hoyland, J.; Saunders, B. R. *Biomacromolecules* **2014**, *15*, 1814.
51. Zhao, J.; Liu, J.; Xu, S.; Zhou, J.; Han, S.; Deng, L.; Zhang, J.; Liu, J.; Meng, A.; Dong, A. *ACS Appl. Mater. Interfaces* **2013**, *5*, 13216.